GENERALIZED INVESTIGATION OF THE ROTATION–ACTIVITY RELATION: FAVORING ROTATION PERIOD INSTEAD OF ROSSBY NUMBER

A. Reiners[1], M. Schüssler[2], and V. M. Passegger[1]
[1] Institut für Astrophysik, Universität Göttingen, Friedrich-Hund-Platz 1, D-37077 Göttingen, Germany
[2] Max-Planck Institut für Sonnensystemforschung, Justus-von-Liebig-Weg 3, D-37077 Göttingen, Germany

ABSTRACT

Magnetic activity in Sun-like and low-mass stars causes X-ray coronal emission which is stronger for more rapidly rotating stars. This relation is often interpreted in terms of the Rossby number, i.e., the ratio of rotation period to convective overturn time. We reconsider this interpretation on the basis of the observed X-ray emission and rotation periods of 821 stars with masses below $1.4\,M_\odot$. A generalized analysis of the relation between X-ray luminosity normalized by bolometric luminosity, $L_{\mathrm{X}}/L_{\mathrm{bol}}$, and combinations of rotational period, P, and stellar radius, R, shows that the Rossby formulation does not provide the solution with minimal scatter. Instead, we find that the relation $L_{\mathrm{X}}/L_{\mathrm{bol}} \propto P^{-2}R^{-4}$ optimally describes the non-saturated fraction of the stars. This relation is equivalent to $L_{\mathrm{X}} \propto P^{-2}$, indicating that the rotation period alone determines the total X-ray emission. Since L_{X} is directly related to the magnetic flux at the stellar surface, this means that the surface flux is determined solely by the star's rotation and is independent of other stellar parameters. While a formulation in terms of a Rossby number would be consistent with these results if the convective overturn time scales exactly as $L_{\mathrm{bol}}^{-1/2}$, our generalized approach emphasizes the need to test a broader range of mechanisms for dynamo action in cool stars.

Key words: dynamo – stars: activity – stars: magnetic field

Online-only material: color figures

1. INTRODUCTION

Stars exhibit signs of magnetic activity through prominent emission of non-thermal radiation from coronal and chromospheric regions (Favata & Micela 2003; Güdel 2004; Hall 2008), and through significant amounts of magnetic flux detectable on their surfaces (Donati & Landstreet 2009; Reiners 2012). It is believed that the chromospheric and coronal regions are magnetically heated and that the generation of magnetic energy by large-scale dynamo action in the stellar convection zone is driven by rotation and convection (e.g., Charbonneau 2010).

The relationship between stellar rotation and activity is extensively discussed in the literature. As soon as the first samples of activity measurements together with information on stellar rotation became available, it was realized that magnetic activity is stronger in rapid rotators while slowly rotating stars (such as the Sun) exhibit relatively low levels of non-thermal emission and host only weak average magnetic fields. Pallavicini et al. (1981) found that the X-ray luminosity, L_{X}, among cool stars (G–M) strongly depends on rotation rate with $L_{\mathrm{X}} \propto (v_{\mathrm{rot}} \sin i)^{1.9\pm0.5}$ and no dependence on bolometric luminosity. The rich data set from the Mt. Wilson survey was used by Noyes et al. (1984) to study the relation between chromospheric activity and rotation. They showed that the ratio of chromospheric flux (observed in Ca II) to bolometric flux correlates with the ratio of a color-dependent function $\tau(B-V)$, which they identified with the convective overturn time, to the rotation period, P. τ/P is proportional to the inverse Rossby number, $1/\mathrm{Ro}$ (sometimes called the Coriolis number), which describes the strength of the rotational effect on the convective flows. Under certain assumptions, the driving of a mean-field $\alpha\Omega$ dynamo is $\propto \mathrm{Ro}^{-2}$ (Durney & Latour 1978; Montesinos et al. 2001), which motivates a scaling of the activity in terms of the Rossby number.

It is clear that comparing τ/P against the ratio of chromospheric or coronal flux to bolometric flux (or luminosity)

involves the possibility that the bolometric flux and overturn time may actually depend on each other in such a way that they cancel each other, and hence this comparison might only reflect the relation between non-thermal flux and rotation period alone, i.e., $L_{\mathrm{X}}/L_{\mathrm{bol}}$ versus τ/P simply reflects the relation L_{X} versus $1/P$. It was pointed out early on, e.g., by Basri et al. (1985) and Basri (1986), that coronal emission and rotation in fact provide a better correlation, or at least that it cannot be decided which one is the relevant relation.

The activity–rotation relationship was re-investigated by Pizzolato et al. (2003) on the basis of a large observational sample of 259 field and cluster stars with known X-ray emission and rotation rates. They showed that two emission regimes exist in cool stars: one for which X-ray luminosity depends on rotation period and a second regime where the ratio between X-ray and bolometric luminosity is constant (called the saturated regime). They also derived an empirical overturn time, τ_{e}, to calculate an empirical Rossby number, $\mathrm{Ro}_{\mathrm{e}} = P/\tau_{\mathrm{e}}$, for their sample stars. The function $\tau_{\mathrm{e}}(B-V)$ was determined such that the scatter in the relation between normalized X-ray luminosity, $L_{\mathrm{X}}/L_{\mathrm{bol}}$, and Ro_{e} is minimized for the non-saturated stars. Similar to Noyes et al. (1984), they found that τ_{e} resembles theoretical overturn timescales. However, they also note that τ_{e} roughly scales as $L_{\mathrm{bol}}^{-1/2}$, which implies that a relation $L_{\mathrm{X}}/L_{\mathrm{bol}} \propto \mathrm{Ro}_{\mathrm{e}}^{-2}$ is equivalent to $L_{\mathrm{X}} \propto P^{-2}$ without any dependence on other stellar parameters.[3] Wright et al. (2011, hereafter W11) extended the available data and presented a sample of 824 cool stars with X-ray luminosities and rotation periods. Similar to Pizzolato et al. (2003), they determined an empirical overturn time by minimizing the scatter between normalized X-ray luminosity and a fit in terms of a power law in the (empirical) Rossby number. For the unsaturated stars in their sample, they found that $L_{\mathrm{X}}/L_{\mathrm{bol}}$ depends on Ro with an exponent of -2.18 ± 0.16

---

[3] Similar results were found for the total Ca II surface flux (Middelkoop 1982; Catalano & Marilli 1983).

if all stars are used. The authors point out that the sample suffers from biases due to the selection of only X-ray detected sources, and they aim to overcome this bias by restricting the fit to an 'unbiased' subsample. From this sample, they found that the slope of the relation between L_X/L_{bol} and Ro has an exponent of -2.70 ± 0.13.

A potential problem of empirically determined convective overturn times is that the physical meaning of this quantity is rather unclear since the overturn time varies with depth and it is not clear at which location the dynamo is most efficient. Furthermore, convective overturn times are likely to depend on other parameters, e.g., metallicity, and change as stars age (e.g., Landin et al. 2010; Spada et al. 2013).

While it is obvious that one can always derive a function τ_e that minimizes the scatter of the activity–rotation relation, it is not clear whether the similarity of the empirical overturn times to those resulting from mixing-length models of convection justifies conclusions concerning the nature of the dynamo process. In this paper, we therefore reduce the freedom of choosing this function by assuming that it is a power law of a fundamental stellar parameter that can, at least in principle, be determined independently for each sample star. For this we choose the stellar radius, R. Similarly, we assume a power law for the dependence of L_X/L_{bol} on the rotational period, P. A fitting procedure based on minimizing scatter then yields optimal values for the two exponents of the power laws for the unsaturated part of the stellar sample. Our main result is that this procedure leads to a better fit of the data (less scatter) than the introduction of the empirical Rossby number. The resulting power-law exponents indicate that $L_X \propto 1/P^2$ in the unsaturated regime. Since L_X is found to be directly related to the magnetic flux on the stellar surface (Pevtsov et al. 2003; Vidotto et al. 2014), this means that the generation of magnetic flux by the stellar dynamo in cool stars is a function only of the rotation period, independent of other stellar parameters (such as radius or mass). Above a critical rotation period, L_X saturates at a level of $10^{-3} L_{bol}$ for each star. Since our results are free from any assumption about the dynamo mechanism, they can be used to assess predictions from dynamo theory in the most general way.

2. DATA

2.1. Stellar Sample

We use the comprehensive sample analyzed by W11. It is based on a compilation started by Pizzolato et al. (2003) and was extended by further data from the literature and from observations of stellar clusters. In total, the sample comprises 824 stars, of which we consider the 821 stars with masses below 1.4 $M_\odot$.

The sample contains stars of very different age, representing the evolution of stars from a few 10^7 years up to the ages of field stars. Specifically, the sample contains members of NGC 2547 (60 stars), IC 2602 (28), IC 2391 (13), α Persei (40), the Pleiades (146), NGC 2516 (14), Praesepe (20), the Hyades (49), as well as 445 field stars. More details on the references for individual measurements together with cluster ages and distances are provided in W11. Here, we adopt the ages collected in that work. In our figures, we distinguish four groups of stellar ages, which we define as very young (up to 50 Myr; NGC 2547, IC 2602, IC 2391), young (between 85 and 150 Myr; α Persei, Pleiades, NGC 2516), intermediate (600–700 Myr; Praesepe and Hyades), and field stars.

Table 1
Updated Rotation Periods

Star	Period (days)		Reference
	Old	Updated	
GJ 182	1.86	4.41	(ks07)
GJ 494	1.54	2.889	(ks07)
GJ 551	42.00	82.53	(ks07)
GJ 2123A	7.79	0.32	(ks07)
GJ 669A	19.81	0.95	(ks07)
HD 95650/GJ410	2.94	14.81	(fh00)
GJ 388/AD Leo	2.6	2.23	(en09)
G99-49	0.5	1.81	(ir11)
GJ 1156	0.87	0.491	(ir11)
GJ 493.1	0.21	0.6	(ir11)
GJ 791.2	0.32	0.346	(ir11)

References. (ks07): Kiraga & Stepien 2007; (fh00): Fekel & Henry 2000; (ir11): Irwin et al. 2011; (en09): Engle et al. 2009.

2.2. Updated Stellar Parameters

2.2.1. Parameters Derived from Models

The catalog of W11 contains measured data for rotation, X-ray luminosity, and color, together with several other indicators. In addition, stellar parameters such as mass, effective temperature, radius, and depth of the convective envelope were calculated from the models of Siess et al. (2000). We updated these parameters by interpolating the tables from Siess et al. (2000), which led in some cases to values that somewhat differ from those given in W11. The discrepancy is most pronounced for the depth of the convective envelope. This is probably due to the fact that the parameter range is poorly covered for masses around $M = 0.35\,M_\odot$ in the tables of Siess et al. (2000). The minimum mass for the appearance of a radiative core is $M = 0.35\,M_\odot$ (Chabrier & Baraffe 1997) and we set the stars to be fully convective for $M \leqslant 0.35\,M_\odot$, thus extending the tabulated points in Siess et al. (2000). For consistency, we also updated the stellar parameter mass, radius, and effective temperature, and we redetermined the bolometric luminosity and used these values for our analysis.

2.2.2. Rotation Periods

For some of the stars in the sample, improved measurements of rotation periods became available in recent years, and some of them significantly differ from those collected in W11. The new periods used for the analysis in this paper are listed in Table 1.

Figure 1 shows an overview of the sample. We plot the rotation period (left) and radius (normalized by the solar radius; right) versus the effective temperature for all sample stars, indicating ages by different colors and symbols. The sample shows the typical signatures of mass-dependent rotational evolution (see, e.g., Barnes & Kim 2010; Reiners & Mohanty 2012).

We note that none of the results shown in the following changes qualitatively if the original stellar parameters and periods from W11 are adopted.

3. RESULTS

3.1. The Generalized Rotation–Activity Relation

We assume that the normalized X-ray luminosity, L_X/L_{bol}, depends on the rotation period and on a combination of parameters given by the structure of the star, such as mass, radius, temperature, or depth of the convection zone. Because
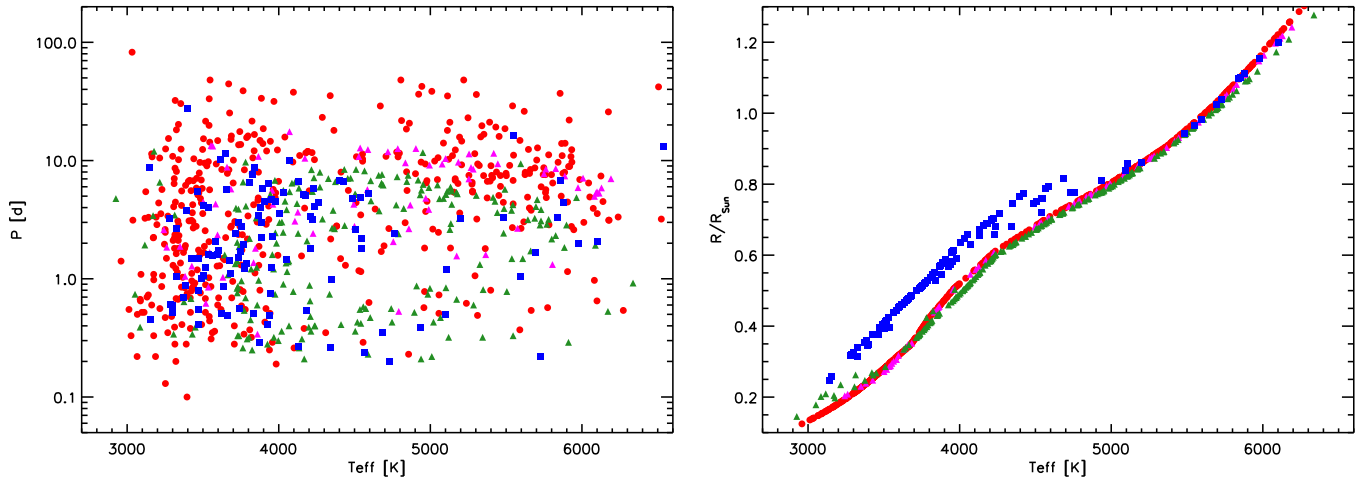
Figure 1. Rotation period (left panel) and radius (right panel) vs. effective temperature for all sample stars. Blue squares: very young stars (up to 50 Myr); green triangles: young stars (between 85 and 150 Myr); magenta triangles: intermediate-age stars (600–700 Myr); red circles: field stars.

(A color version of this figure is available in the online journal.)

they all scale in some way with the mass or the radius of the star, we condense the dependence on stellar parameters in the radius R, and search for an optimal representation that minimizes the scatter in L_X/L_{bol}. For a generalized dependence of L_X/L_{bol} on P and R in the form of a combination of power laws,

$$\frac{L_X}{L_{bol}} \propto R^\alpha P^\beta, \qquad (1)$$

we considered fits through the resulting distributions of points in the plane $\log(L_X/L_{bol})$ versus $\log(k R^\alpha P^\beta)$, where k represents the constant of proportionality in Equation (1). The fit curves are composed of two linear parts: one for the unsaturated regime, which should follow the relationship given by Equation (1) and therefore must have a slope of unity; and another linear fit for the saturated part of the sample. The best fit is then defined as the one showing the minimum scatter of the data points with respect to the fit curve. The location of the break in the slope of the fit curve between the unsaturated and saturated parts is found by including the break point in the minimization process.

The linear regression curves are calculated using an adapted version of a procedure studied by Isobe et al. (1990), who provide algorithms for five methods for linear regression fits to bivariate data.[4] The different methods are useful for taking into account different distributions of uncertainties in the data. The "standard" way of fitting a slope in a variable Y to another variable X is the ordinary least squares method, OLS $(Y|X)$. This method assumes that Y measures (with uncertainty) the value of a parameter that depends on a known variable X (with no or very little uncertainty). A second method, OLS $(X|Y)$, calculates the fit under the assumption that Y is the variable that is well defined and the scatter in the observed sample is due to a distribution (or measurement uncertainties) in X. A third method, the OLS bisector, performs the fit under the assumption that the scatter in the distribution is due to scatter in both variables X and Y with symmetrically distributed scatter. This relation provides the regression that produces the "best-looking" fit, i.e., a line that lies closest to all data points. In our situation, typical uncertainties in the variables X and Y are not symmetric. The intrinsic scatter in L_X of a Sun-like star due to stellar variability is typically on the order of a factor of two but higher during flare

events (Schmitt et al. 1995). Uncertainties in L_{bol} and differences between X-ray calibrations from different instruments can add more uncertainty so that a factor of two is probably a lower limit for the uncertainty in L_X/L_{bol} in our sample. Stellar radii are derived in a consistent way, so that residual errors are probably only a few percent. The rotation periods in the sample are also relatively well constrained. We do not expect any systematic differences between periods measured by different authors, and the variability of observed rotation periods in Sun-like stars is reported to be on the order of 10%–20% or lower (Donahue et al. 1996), i.e., the uncertainty in our variable X is a factor of 10–20 less than the uncertainty in our variable Y. Thus, we conclude that OLS $(Y|X)$ is the appropriate method for the calculation in our case. We thereby ignore the uncertainty in P, which probably leads to a slight underestimate of the slope (Isobe et al. 1990). We estimate this effect to be less than 0.1 from tests using the OLS $(Y|X)$ and OLS bisector methods.

For the optimal solution with a scatter of 0.346 dex, we find values of $\alpha = -4.3$, $\beta = -2.2$, $k = 1.86 \times 10^{-3}$ d$^{-\beta}$ $R_\odot^{-\alpha}$, and the break point at $\log(L_X/L_{bol}) = \log(k R^\alpha P^\beta) = -3.14$. Up to three digits, the scatter is also the same for the combination $\alpha = -4$ and $\beta = -2$. For simplicity, we will consider these values as our optimal solution in what follows.[5]

In order to determine a confidence interval for the optimal solution, we note that the nature of the assumed power-law relationship in the unsaturated part implies that the scatter of the data points around Equation (1) on the log-log plane, and hence the quality of the fit, depends only on the ratio of the exponents, α/β. We thus calculated the scatter as a function of α/β by determining the standard deviation of the data points from the broken power-law fit, using the value of the break point that minimizes the standard deviation for each given value of α/β. We carried out this procedure for 101 values for each of the parameters α and β with $-6 \leqslant \alpha \leqslant 0$ and $-6 \leqslant \beta \leqslant 0$. The resulting relation between the scatter (in dex) and α/β is shown in Figure 2. We find a smooth distribution with a minimum located at $\alpha/\beta = 1.93$ (2.06 for the original sample). We estimate a confidence interval of this solution assuming that

---

[4] http://idlastro.gsfc.nasa.gov/ftp/pro/math/sixlin.pro

[5] For the original sample, i.e., if we use all periods and luminosities reported in W11, we find $\alpha = -4.1$, $\beta = -2.0$, $k = 1.23 \times 10^{-3}$ d$^{-\beta}$ $R_\odot^{-\alpha}$, and the break point at $\log(L_X/L_{bol}) = \log(k R^\alpha P^\beta) = -3.20$.
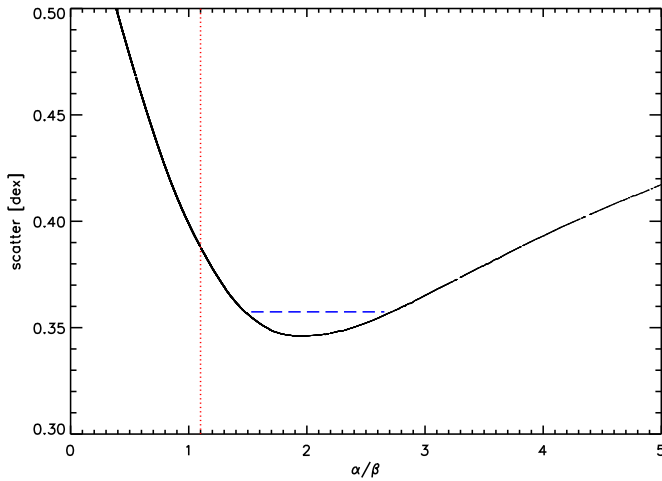
Figure 2. Scatter (1σ) of L_X/L_{bol} around Equation (1) for different values of the ratio α/β. The blue dashed line marks the 2σ interval for α/β assuming that the statistical uncertainty in the measurement of L_X/L_{bol} equals the minimum scatter of 0.346 dex. The red dotted line shows the approximate location derived in W11 from the Rossby formulation based on their "unbiased" subsample of stars (see text).

(A color version of this figure is available in the online journal.)

the uncertainties in L_X/L_{bol} follow a normal distribution around our fit. In other words, we assume that the uncertainty of each individual measurement is equal to the minimum of the scatter. With a minimum scatter of 0.346 dex and a total number of 349 measurements of stars in the unsaturated regime, we estimate (see Press et al. 1986) as the 2σ confidence interval of the ratio α/β the range

$$1.53 < \frac{\alpha}{\beta} < 2.66, \qquad (2)$$

which is indicated by the blue dashed line in Figure 2. For the individual values of α and β, we find the 2σ intervals

$$-5.04 < \alpha < -3.54, \qquad (3)$$

and

$$-2.37 < \beta < -1.88. \qquad (4)$$

We note that the assumption of normally distributed uncertainties in the individual measurements of L_X/L_{bol} is probably not entirely correct. Nevertheless, a 1σ uncertainty of 0.346 dex (more than a factor of two) appears to be a realistic estimate that captures several systematic effects, such as instrument differences, flares (occurring statistically), and contamination from binaries. Ratios outside the confidence interval can therefore be regarded as statistically unlikely, even if we do not fully understand the sources of the measurement uncertainties. The dotted red vertical line in Figure 2 indicates the value of $\alpha/\beta = 1.1$ that we infer for the formulation of W11 in terms of the Rossby number (see Section 3.2 below); it is clearly outside the 2σ confidence interval.

Our result provides information on the dependence between the parameters used in Equation (1). It is important to note that in the available sample, rotation, color, mass, radius, age, etc., are severely degenerate, for example, because very few Sun-like stars are rapidly rotating. Our result is that the rotation period, P, and radius, R, can explain the existing activity observations but underlying physical relations may be hidden by sample degeneracies. Further data on stars occupying sparsely populated parameter ranges would help to remove this degeneracy.

Table 2
Slope γ in the Unsaturated Regime for the Three Cases in W11

Sample	OLS ($Y\|X$)	OLS bisector	OLS ($X\|Y$)
$0.13 <$ Ro	-2.16 ± 0.08	-2.58 ± 0.08	-3.17 ± 0.12
$0.2 <$ Ro < 3.0	-2.36 ± 0.09	-2.90 ± 0.09	-3.71 ± 0.17
"unbiased" sample[a]	-1.91 ± 0.18	-2.24 ± 0.16	-2.67 ± 0.25

Note. [a] Valid in the range $0.3 <$ Ro < 3; HD 81809 is not in the catalog.

3.2. Comparison to Wright et al. (2011)

Wright et al. used the same sample of stars to obtain a power-law relation between L_X/L_{bol} and an empirical Rossby number by considering the convective overturn time, τ, as an adjustable function of stellar mass. By minimizing the scatter of the data points with respect to the power-law fit, they determined the slope γ in

$$\frac{L_X}{L_{bol}} \propto \left(\frac{P}{\tau}\right)^\gamma \qquad (5)$$

in the unsaturated regime. Including all 824 stars in their sample, they report $\gamma = -2.18 \pm 0.16$ for the best-fitting slope. The authors argue that an OLS bisector fit is appropriate for this sample. We question this choice because of the asymmetric distribution of the uncertainties (see Section 3). To compare the results from different fit methods, we recalculated the slope using three different methods: OLS ($Y|X$), OLS bisector, and OLS ($X|Y$). The results are shown in Table 2.[6] We include three subsamples that are mentioned in W11, the full sample (with Ro > 0.13), a sample with Ro > 0.2, and their "unbiased" sample (see below). We observe rather large inconsistencies between our results and their findings, which may be partly because we cannot reconstruct the overturn times W11 used for their fit. These overturn times follow the relation from Pizzolato et al. (2003), but W11 convert $V - K$ into $B - V$ based on a relation that is not provided for all stars. We therefore used the convective overturn times as determined in W11 as a function of mass, which do not significantly differ from those of Pizzolato et al. as shown in W11.

An important point in the results from W11 is their construction of an "unbiased" sample. The authors argue that X-ray bright sources are easier to detect and may therefore be over-represented with respect to stars that are X-ray dim. This could be particularly important for the mean L_X for a given value of P because slow rotators with low X-ray brightness may be systematically underrepresented. To construct an X-ray complete sample, they chose the 36 stars from Donahue et al. (1996) for which rotation periods could be measured over five or more seasons. According to W11, the 36 stars all show measurable X-ray emission and W11 argue that the sample therefore does not suffer from X-ray luminosity bias.[7] We do not agree that this particular sample should be less biased than others, in particular because it is a sample of 36 selected out of 100 stars based on the detectability of photometric periods. We calculated the slope for this sample and include our results in Table 2. We cannot reproduce the value of $\gamma = -2.7$ for the OLS bisector method. We revisit the question of luminosity bias in Section 3.6.

---

[6] For this comparison, we use the original values for P and L_X as reported in W11.
[7] We note that HD 81809 is a member of the 36 stars from Donahue et al. (1996), but we could not find it in either the sample of W11 or in the NEXXUS database (Liefke & Schmitt 2005).
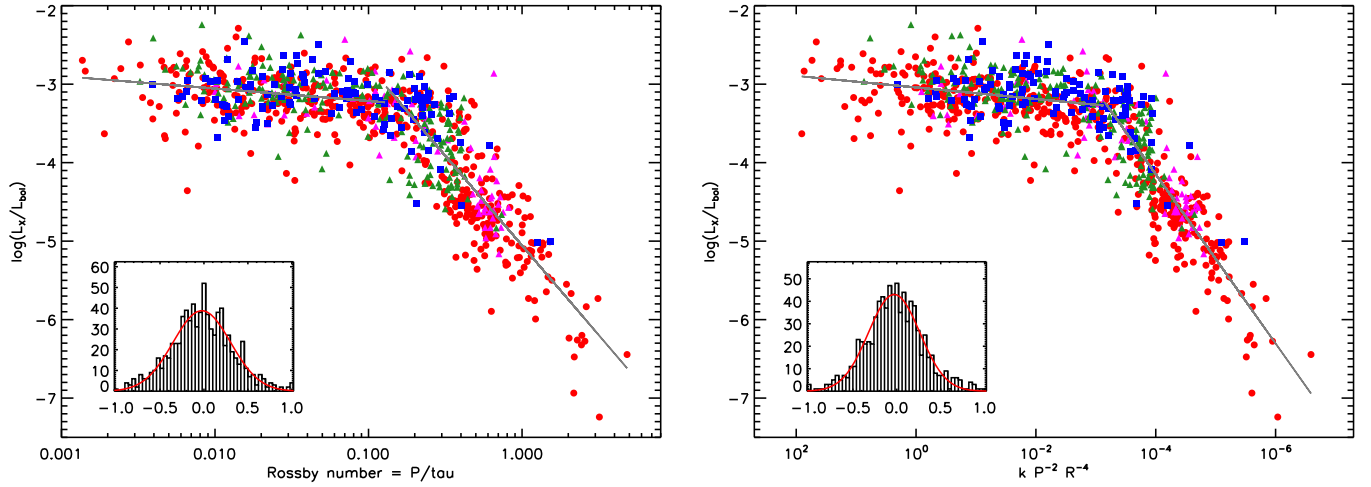
Figure 3. Normalized X-ray luminosity as a function of empirical Rossby number (left) and as a function of $k P^{-2} R^{-4}$ (right). Different colored symbols show stars at different ages (see Figure 1). The distributions are fit using a broken power law (gray lines) with the break at Ro = 0.13 (left panel) and $\log k P^{-2} R^{-4} = -3.14$ (right panel). Scatter around the fit is shown in the inset of each panel, a Gauss fit is overplotted in each panel's inset as a red line.

(A color version of this figure is available in the online journal.)

For completeness, we compare the scaling reported in W11 ($\gamma = -2.7$) to our solution. We note that this is not comparing the same samples, but we find it helpful to discuss the $\gamma = -2.7$ scaling to our generalized results. The convective overturn time for the W11 solution was parameterized in terms of stellar mass, M, by a second-order double-logarithmic polynomial (see their Equation (11)). For the stars considered in the unsaturated part of the sample, the values of $M/M_\odot$ and $R/R_\odot$ are almost identical, so that we can replace $M/M_\odot$ in their relation by $R/R_\odot$ without introducing significant scatter. Furthermore, we can approximate their Equation (11) by the first-order relation

$$\log \tau = 1.19 - 1.08 \log M/M_\odot, \qquad (6)$$

so that we can rewrite Equation (5) in the form

$$\frac{L_X}{L_{bol}} \propto \left(\frac{R^{-1.08}}{P} \right)^{2.7} = P^{-2.7} R^{-2.9}, \qquad (7)$$

which is equivalent to Equation (1) with $\alpha/\beta = 2.9/2.7 = 1.1$. This value is indicated by the red dotted line in Figure 2; it is outside the 2σ confidence interval for the optimal value of α/β. The expected scatter for $\alpha/\beta = 1.1$ is approximately 0.38 dex. A more direct comparison of the fit qualities can be achieved if we use the original Rossby scaling provided by W11 and compare its scatter to the one determined from the distribution using $\alpha = -4$ and $\beta = -2$. In Figure 3, we show the normalized X-ray luminosity as a function of the Rossby number (left panel) and as a function of $k P^{-2} R^{-4}$ for minimal scatter (right panel). In both panels, we overplot broken power-law fits to the data. For the values from W11, we break the power law at $Ro_{sat} = 0.13$, as reported in that work. For the values of k and the power-law break in the $\alpha = -4$ and $\beta = -2$ solution, we take the values of the optimal solution.

From both descriptions, we determined the scatter around the power-law fit by calculating the standard deviations of the distributions shown in the insets of the panels of Figure 3. For the Rossby formulation, the standard deviation is $\sigma = 0.371$ dex, while for the generalized formulation (right panel in Figure 3) we have $\sigma = 0.346$ dex (as found in Section 3.1). Compared to the simplified approach using Equation (6), the value for the optimized Rossby formulation is closer to, but still considerably higher than, the minimum from our generalized formulation.

3.3. Comparison to Pizzolato et al. (2003)

A quadratic dependence of X-ray luminosity on rotation rate alone was already suggested by Pallavicini et al. (1981). More recently, Pizzolato et al. (2003) pointed out that the empirical turnover time approximately scales as $\tau \propto L_{bol}^{-1/2}$. With a rotation–activity relation of the form $L_X/L_{bol} \propto \mathrm{Ro}^{-2}$, they then obtain

$$\frac{L_X}{L_{bol}} \propto \mathrm{Ro}^{-2} \propto \frac{1}{P^2 L_{bol}}, \qquad (8)$$

which is equivalent to $L_X \propto P^{-2}$. This relation is consistent with the result of our generalized approach, which can be seen as follows. Since $L_{bol} \propto R^2 T_{eff}^4$, and for the non-saturated stars approximately $T_{eff} \propto R^{1/2}$, with $\alpha = -4$ and $\beta = -2$ we find the relation

$$\frac{L_X}{L_{bol}} \propto P^{-2} R^{-4} \propto \frac{1}{P^2(R^2 T^4)} \propto \frac{1}{P^2 L_{bol}}, \qquad (9)$$

which is identical to the relation in Equation (8). The factor of R^{-4} effectively compensates for the normalization by the bolometric luminosity, indicating that the normalization is in fact unwarranted in the unsaturated regime.

Since we have the values of L_{bol} for the stars in our sample, we can also directly consider the relation $L_X/L_{bol} \propto 1/(P^2 L_{bol})$. It turns out that the scatter from this relation is 0.340 dex, which is even slightly lower than the minimum scatter of 0.346 dex for the relation given in Equation (1). This supports the conclusion that the relation between L_X and P^{-2} is better constrained than the relation between L_X/L_{bol} and some combination of P and other stellar parameters.

3.4. Saturation

We have seen that the total X-ray luminosity in the unsaturated regime scales with P^{-2} and does not depend on any other stellar parameter. When the total X-ray luminosity reaches a critical value of about $10^{-3} L_{bol}$, it does not grow further for shorter rotational periods, i.e., activity saturates. The critical period at which saturation sets in therefore depends on the stellar luminosity, L_{bol}. We can use our optimal solution to determine the value of the critical period. For $\alpha = -4$,
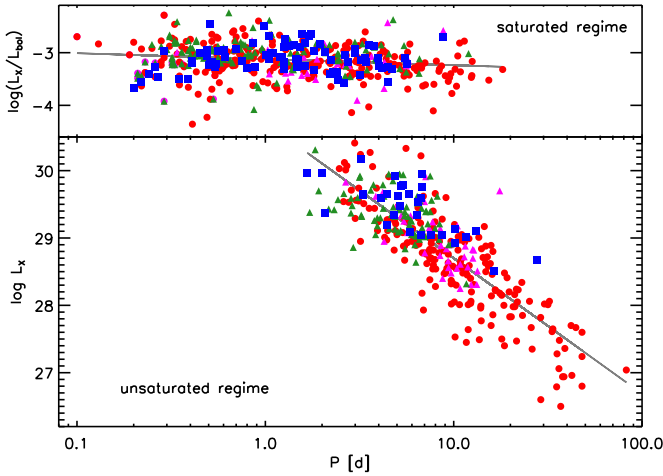
Figure 4. Separate representations of X-ray activity vs. rotation period in the unsaturated (lower part) and saturated (upper part) regimes. Activity is represented in terms of L_X in the unsaturated regime and in terms of L_X/L_{bol} in the saturated regime.

(A color version of this figure is available in the online journal.)

$\beta = -2$, and $k = 1.86 \times 10^{-3} \, d^2 \, R_\odot^4$, saturation sets in at about $\log k P^{-2} R^{-4} = -3.14$. With $L_{bol} \propto R^4$ and $L_\odot = 3.853 \times 10^{33} \, erg \, s^{-1}$, we find

$$P_{sat} \, (days) = 1.6 \left(\frac{L_{bol}}{L_\odot} \right)^{-1/2} = \left(\frac{L_{bol}}{1.1 \times 10^{34}} \right)^{-1/2}, \quad (10)$$

where L_{bol} is in units of $erg \, s^{-1}$. This result is similar to Equation (6) of Pizzolato et al. (2003).

For this value of the critical period, we show the distribution of $\log L_X$ versus P for the unsaturated regime together with $\log(L_X/L_{bol})$ versus P for the saturated regime in the lower and upper panels of Figure 4, respectively. For the unsaturated regime, we find the relation

$$\log L_X = (30.71 \pm 0.05) - (2.01 \pm 0.05) \log P, \quad (11)$$

which is consistent with our optimal value $\beta = -2$.[8]

3.5. A Slope in the Saturated Regime

All three representations shown in Figures 3 and 4 indicate a slight slope of the rotation–activity relationship in the saturated regime, i.e., some remnant dependence of the activity on rotation (or other parameters) even for very rapidly rotating stars. Quantitatively, we find the following for the different representations:

$$\log \frac{L_X}{L_{bol}} = (-3.37 \pm 0.06) - (0.16 \pm 0.03) \log Ro,$$

$$\log \frac{L_X}{L_{bol}} = (-3.04 \pm 0.02) - (0.07 \pm 0.01) \log (k P^2 R^4),$$

$$\log \frac{L_X}{L_{bol}} = (-3.12 \pm 0.01) - (0.11 \pm 0.03) \log P.$$

There is a statistically significant slope in all three cases. The slope is least significant (but still above 3σ) in the parameterization with P, while it is at $\geqslant 5\sigma$ and more in the other two cases. The slope is likely due to a remaining dependence of the dynamo on rotation period even when saturation is reached, but it may also be influenced by small differences in the saturation level between stars of different mass.

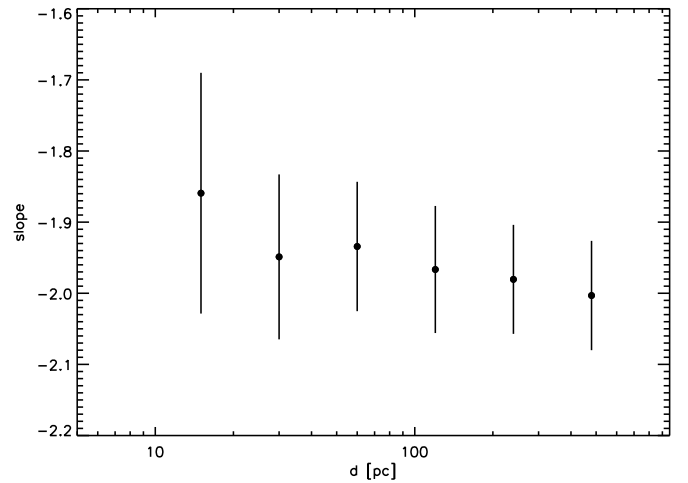
[8] For the original sample, we find $\beta = 1.97 \pm 0.08$.

Figure 5. Slope β for subsamples that contain stars out to a maximum distance. Error bars show 1σ uncertainties.

3.6. Luminosity Bias

W11 pointed out that the slope of the rotation–activity relation may suffer from a luminosity bias. A possible consequence is that the least X-ray bright stars are systematically missed, so that the average X-ray luminosity among the least active stars (the slowest rotators) is overestimated. This would lead to a slope that is shallower than the true relation. We lack a statistically unbiased, complete sample of stars with X-ray and rotation period measurements. Nevertheless, the large sample of targets allows us to test whether the slope β that we derive in the unsaturated regime depends on the distance to the stars in the sample. A luminosity bias would be less pronounced in a sample of nearby stars and would become more important if we include increasingly distant objects. We carried out this test by computing the slope β for stars in the sample with distances out to 15, 30, 60, 120, 240, and 480 pc. The results are shown in Figure 5. We find no significant trend of β as a function of distance limit. There is a marginal trend towards *higher* absolute values of the slope at large distances, but it is dominated by the sample limited to 15 pc which has large uncertainties. We conclude that our results do not show evidence of a luminosity bias.

4. DISCUSSION

The result of our generalized analysis of the rotation–activity relation can be summarized as follows. The total X-ray luminosity scales with the rotation period (P^{-2}) as long as the stellar activity is not saturated, and X-ray activity saturates for a given star when L_X/L_{bol} reaches a level of about 10^{-3}. In the unsaturated regime, this description is equivalent to a scaling of $L_X/L_{bol} \propto P^{-2} R^{-4}$, which could be written as a Rossby number scaling of the form $L_X/L_{bol} \propto Ro^{-2}$ if the convective overturn time scales as $\tau \propto R^{-2} \propto L_{bol}^{-1/2}$. Furthermore, for a given star in the saturated regime, L_X/L_{bol} still shows a weak but significant dependence on rotation. In what follows, we discuss some physical implications of these results.

4.1. $L_X \propto P^{-2}$

This relationship means that two stars with the same rotation period emit the same X-ray luminosity, irrespective of their mass or radius. Since observations indicate that L_X is proportional to Φ_s, the total magnetic flux at the stellar surface (Pevtsov et al.

2003), this implies that Φ_s depends only on the rotation rate and not on any other stellar parameter. This is consistent with a recent study by Vidotto et al. (2014) of the relationship between the large-scale surface magnetic flux determined by Zeeman Doppler Imaging, Φ_V, and X-ray luminosity: the two relations, L_X versus Φ_V, and L_X/L_{bol} versus Φ_V, yield nearly the same power-law exponents (1.80 and 1.82, respectively). This means that Φ_V is uncorrelated with L_{bol} and, therefore, uncorrelated with stellar radius or mass. Similarly, the scalings with a rotation period of Φ_V and magnetic flux density (Φ_V divided by surface area) show the same power-law exponent, which means that the rotation rate is uncorrelated with radius or mass (consistent with our value $\alpha = -4$).

The absence of a dependence of L_X on stellar parameters apart from rotation means that a bigger star shows the same magnetic surface flux as a smaller star at the same rotation rate. One would have naively expected that the bigger volume of the convection zone available for dynamo action would also lead to more magnetic flux being produced by the dynamo, so that more flux also emerges at the surface. Also, bigger scales could imply less dissipation of the large-scale field by turbulent diffusion, thus effectively increasing the net driving of the dynamo. On the other hand, the turbulent magnetic diffusivity probably decreases towards cooler (smaller) stars since the convective motions are slower; the net effect on dynamo driving is unclear.

4.2. Saturation

The existence of a limiting value $L_X/L_{bol} \approx 10^{-3}$ for very fast rotators lends itself to at least three possible interpretations.

First, it can be seen as indicating that there is a maximum fraction of the total energy flux of the star that can be converted into X-ray flux. This could be related to an upper limit of the efficiency of converting the energy flux into magnetic energy (e.g., Reiners et al. 2009; Christensen et al. 2009), although the relation between the X-ray flux and magnetic energy generation in the convection zone is unclear.

A second possible interpretation can be inferred from the scaling of the critical rotation period for saturation given in Equation (10): $P_{sat} \propto L_{bol}^{-1/2} \propto R^{-2}$. This relation implies that the critical rotation rate, $2\pi/P_{sat}$, is proportional to the surface area of the star, so that it can be interpreted as the rotation rate at which the magnetic surface flux in bipolar regions fills the complete stellar surface (e.g., Vilhu 1984). If the X-ray flux ultimately results from the interaction of surface magnetic flux with near-surface flows, saturation could be a result of this situation. In this picture, the filling of the surface would also need to imply that the total surface magnetic flux is saturated, evidence of which is reported in Reiners et al. (2009). For a solar-type star, saturation occurs at $L_X \approx 4 \times 10^{30}$ erg s^{-1}, roughly a factor of 10^3 above the value at the activity maxima of the Sun today, during which the area fraction of the active regions is a few percent. For $L_X \propto \Phi_s$ (Pevtsov et al. 2003), the saturated X-ray luminosity would not be reached for a Sun fully covered by active regions (e.g., Vaiana & Rosner 1978; Drake et al. 2000); however, it would be consistent for a steeper relationship, such as $L_X \propto \Phi_s^{1.8}$ proposed by Vidotto et al. (2014).

Another interpretation can be given in terms of the nonlinearities that determine the amplitude of the dynamo-generated magnetic field (R.H. Cameron 2014, private communication). The present Sun is located in the lower part of the unsaturated regime and its differential rotation is almost invariant during the activity cycle. This means that the magnetic energy is small compared to the kinetic energy in the differential rotation, which therefore does not experience a strong back reaction of the toroidal magnetic field it generates. The field amplitude in the unsaturated regime is thus determined by a nonlinearity affecting the generation of the poloidal field (α quenching). As the rotation rate grows along the unsaturated branch, at some stage the magnetic energy becomes comparable to the kinetic energy of differential rotation so that a strong back reaction occurs ("Ω quenching"). If the corresponding nonlinearity is sufficiently hard, it results in a quasi-saturated regime that is (almost) independent of the rotation rate.

4.3. Dynamo Models

Given the present state of our understanding of solar and stellar dynamos (see, e.g., Charbonneau 2010), drawing a quantitative connection between the dynamo mechanism and the observed activity indices is by no means straightforward. It seems uncontroversial that the toroidal flux is generated (from poloidal flux) by differential rotation (the Ω effect) while the poloidal flux is regenerated by some kind of α effect. The latter could be due to the action of cyclonic convection on the toroidal field, i.e., the classical Parker loop, which would bring the Rossby number into consideration. However, it could also result from the Babcock–Leighton mechanism, i.e., the systematic tilt of bipolar regions with respect to the direction of rotation. This tilt can result from the action of the Coriolis force on flows along rising flux tubes (Fan 2009). These flows are not of a convective nature, and thus are independent from a Rossby number.

The combination of α effect and Ω effect provides the driving of the dynamo, but the relation of this driving to rotation is uncertain. Since the α effect is due to the action of the Coriolis force, one can argue that it should be proportional to the rotation rate, at least for not-too-rapid rotation. The relation of differential rotation to the overall rotation rate is much more unclear, so that the scaling of dynamo driving (expressed by a non-dimensional dynamo number involving the product of α and Ω effect) with rotation is rather uncertain. The dependence on other stellar parameters is unclear as well and mostly addressed by crude dimensional arguments.

The scaling of the amplitude of the dynamo-generated field with the driving dynamo number depends crucially on the kind of nonlinear back reaction of the magnetic field on its sources, which limits the growth of the magnetic energy. There are various nonlinearities that could play a role here, e.g., quenching of the α effect and differential rotation, flux loss by magnetic buoyancy, and driving of large-scale flows, all of which are not well understood quantitatively. As a consequence, dynamo models mostly consider them in an ad hoc fashion. Keeping in mind these severe uncertainties, it is interesting to note that at least some models show roughly similar dependencies of the field amplitude on the dynamo driving (dynamo number, N_D): $\propto N_D^{1/2}$ for simple one-dimensional models (Stix 1972; Schmitt & Schüssler 1989), and $\propto N_D^{0.65}$ for a state of the art two-dimensional flux-transport dynamo model (Karak et al. 2014); the latter is also consistent with the result from an earlier model by Jouve et al. (2010). However, quite different dependencies are found with other models (e.g., Robinson & Durney 1982) and a dynamo model with an α effect and differential rotation taken from global three-dimensional simulations even fails to show an increase of activity with rotation rate (Dubé & Charbonneau 2013).

Eventually, the observed activity indices (such as L_X) are related to the surface flux emerging in bipolar magnetic regions.

How this flux is connected quantitatively with the general dynamo amplitude, i.e., the amount of magnetic flux or magnetic energy generated in the convection zone, depends on the detailed processes leading to flux emergence. Again, these processes are not well understood and different mechanisms are possible: instability of strong magnetic flux tubes (Fan 2009) or buoyant local flux concentrations compressed to super-equipartition by turbulent convective flows (Nelson et al. 2011, 2014).

5. CONCLUDING REMARKS

We used activity and rotation measurements of 821 stars, compiled in the sample of W11, to perform a generalized analysis of the rotation–activity relation. The sample was updated with recent period measurements from the literature. We considered the relation of normalized X-ray luminosity, L_X/L_{bol}, to rotation period, P, and stellar parameters condensed in the radius, R, in the functional form $R^\alpha P^\beta$. In the unsaturated regime, we found the representation with the least scatter for $\alpha = -4$ and $\beta = -2$. Since approximately $L_{bol} \propto R^4$, this solution is equivalent to $L_X \propto P^{-2}$, a relation that had already been found by Pallavicini et al. (1981) and Pizzolato et al. (2003). On the other hand, the most recent parameterization of the activity–rotation relation in terms of the Rossby number by W11 does show a significantly higher scatter.

In the subsample of stars that are in the saturated regime, we found a slight but significant growth of L_X/L_{bol} with faster rotation. It is unclear whether this trend is due to an effect of P beyond the saturation limit or results from a degeneracy between stellar mass and rotation rate reflecting that L_X/L_{bol} is slightly larger for more luminous stars.

Formally, we can rewrite $R^{-4}P^{-2}$ in terms of a Rossby number, $Ro = P/\tau$, if the convective overturn time scales as $\tau \propto R^{-2} \propto L_{bol}^{-1/2}$. We then obtain $L_X/L_{bol} \propto Ro^{-2}$. Unless we have a reliable determination of the Rossby number in stellar convection zones (provided that this is possible at all), we cannot decide whether the physical mechanism behind the rotation–activity relation is better represented by a Rossby-number scaling of L_X/L_{bol} or by a purely rotational scaling of L_X independent of other stellar parameters. However, since the latter involves no assumptions on physical conditions to be valid in the star, we favor this description and find it unnecessary to explain the rotation–activity relation in terms of the Rossby formulation.

The dependence of dynamo driving (as possibly expressed by a dynamo number), its nonlinearity, and the amount of magnetic flux emerging at the stellar surface on rotation and other stellar parameters (such as radius) is quite unclear. The various factors may well combine for a result that makes the surface flux independent of stellar radius as indicated by our analysis. One possible method to condense this independence into a physical model is to assume a Rossby scaling with a convective overturn time that is (exactly) proportional to the square-root of the stellar luminosity. One can think of many other families of models that can potentially lead to this result, and this opens room for more general descriptions of the magnetic dynamo.

REFERENCES

Barnes, S. A., & Kim, Y.-C. 2010, ApJ, 721, 675
Basri, G. 1986, in Lecture Notes in Physics, Cool Stars, Stellar Systems and the Sun, Vol. 254, ed. M. Zeilik & D. M. Gibson (Berlin: Springer), 184
Basri, G., Laurent, R., & Walter, F. M. 1985, ApJ, 298, 761
Catalano, S., & Marilli, E. 1983, A&A, 121, 190
Chabrier, G., & Baraffe, I. 1997, A&A, 327, 1039
Charbonneau, P. 2010, LRSP, 7, 3
Christensen, U. R., Holzwarth, V., & Reiners, A. 2009, Natur, 457, 167
Donahue, R. A., Saar, S. H., & Baliunas, S. L. 1996, ApJ, 466, 384
Donati, J.-F., & Landstreet, J. D. 2009, ARA&A, 47, 333
Drake, J. J., Peres, G., Orlando, S., Laming, J. M., & Maggio, A. 2000, ApJ, 545, 1074
Dubé, C., & Charbonneau, P. 2013, ApJ, 775, 69
Durney, B. R., & Latour, J. 1978, GApFD, 9, 241
Engle, S. G., Guinan, E. F., & Mizusawa, T. 2009, in AIP Conf. Proc. 1135, Future Directions in Ultraviolet Spectroscopy: A Conference Inspired by the Accomplishments of the Far Ultraviolet Spectroscopic Explorer Mission, ed. M. E. van Steenberg et al. (Melville, NY: AIP), 221
Fan, Y. 2009, LRSP, 6, 4
Favata, F., & Micela, G. 2003, SSRv, 108, 577
Fekel, F. C., & Henry, G. W. 2000, AJ, 120, 3265
Güdel, M. 2004, A&ARv, 12, 71
Hall, J. C. 2008, LRSP, 5, 2
Irwin, J., Berta, Z. K., Burke, C. J., et al. 2011, ApJ, 727, 56
Isobe, T., Feigelson, E. D., Akritas, M. G., & Babu, G. J. 1990, ApJ, 364, 104
Jouve, L., Brown, B. P., & Brun, A. S. 2010, A&A, 509, A32
Karak, B. B., Kitchatinov, L. L., & Choudhuri, A. R. 2014, ApJ, 791, 59
Kiraga, M., & Stepien, K. 2007, A&A, 57, 149
Landin, N. R., Mendes, L. T. S., & Vaz, L. P. R. 2010, A&A, 510, A46
Liefke, C., & Schmitt, J. H. M. M. 2005, in ESA Special Publication, Vol. 560, 13th Cambridge Workshop on Cool Stars, Stellar Systems and the Sun, ed. F. Favata, G. A. J. Hussain, & B. Battrick (Noordwijk: ESA), 755
Middelkoop, F. 1982, A&A, 107, 31
Montesinos, B., Thomas, J. H., Ventura, P., & Mazzitelli, I. 2001, MNRAS, 326, 877
Nelson, N. J., Brown, B. P., Brun, A. S., Miesch, M. S., & Toomre, J. 2011, ApJL, 739, L38
Nelson, N. J., Brown, B. P., Sacha Brun, A., Miesch, M. S., & Toomre, J. 2014, SoPh, 289, 441
Noyes, R. W., Hartmann, L. W., Baliunas, S. L., Duncan, D. K., & Vaughan, A. H. 1984, ApJ, 279, 763
Pallavicini, R., Golub, L., Rosner, R., et al. 1981, ApJ, 248, 279
Pevtsov, A. A., Fisher, G. H., Acton, L. W., et al. 2003, ApJ, 598, 1387
Pizzolato, N., Maggio, A., Micela, G., Sciortino, S., & Ventura, P. 2003, A&A, 397, 147
Press, W. H., Flannery, B. P., & Teukolsky, S. A. 1986, Numerical Recipes. The Art of Scientific Computing (Cambridge: Cambridge Univ. Press)
Reiners, A. 2012, LRSP, 9, 1
Reiners, A., Basri, G., & Browning, M. 2009, ApJ, 692, 538
Reiners, A., & Mohanty, S. 2012, ApJ, 746, 43
Robinson, R. D., & Durney, B. R. 1982, A&A, 108, 322
Schmitt, D., & Schüssler, M. 1989, A&A, 223, 343
Schmitt, J. H. M. M., Fleming, T. A., & Giampapa, M. S. 1995, ApJ, 450, 392
Siess, L., Dufour, E., & Forestini, M. 2000, A&A, 358, 593
Spada, F., Demarque, P., Kim, Y.-C., & Sills, A. 2013, ApJ, 776, 87
Stix, M. 1972, A&A, 20, 9
Vaiana, G. S., & Rosner, R. 1978, ARA&A, 16, 393
Vidotto, A. A., Gregory, S. G., Jardine, M., et al. 2014, MNRAS, 441, 2361
Vilhu, O. 1984, A&A, 133, 117
Wright, N. J., Drake, J. J., Mamajek, E. E., & Henry, G. W. 2011, ApJ, 743, 48 (W11)